Research article

# Electroacupuncture improves low-grade duodenal inflammation in FD rats by reshaping intestinal flora through the NF-κB p65/ NLRP3 pyroptosis pathway

Yong-Li Han [a], Zhao-Xia Kang [b], Shu-Wen Jin [c], Xiao-Li Pan [c], Hong-Xing Zhang [c,d,e], Liang-Yu Zhang [f], Lei Tang [g,*]

[a] *Acupuncture Department, The First Affiliated Hospital of Henan University of CM, Zhengzhou, Henan, 450003, China*
[b] *Department of Acupuncture and Moxibustion, GuiZhou University of Traditional Chinese Medicine, GuiYang, GuiZhou, 550025, China*
[c] *College of Acupuncture and Orthopedics, Hubei University of Chinese Medicine, Wuhan, Hubei, 430061, China*
[d] *Jianghan University Health Science Center, Wuhan, Hubei, 430056, China*
[e] *Institute of Acupuncture and Moxibustion, Jianghan University, Wuhan, Hubei, 430056, China*
[f] *Digestive Endoscopy Treatment Center, Second Affiliated Hospital, Nanjing University of Chinese Medicine, Nanjing, Jiangsu, 210017, China*
[g] *Rehabilitation Department, Central Hospital of Wuhan, Tongji Medical College, Huazhong University of Science and Technology, Wuhan, Hubei, 430014, China*

## ARTICLE INFO

## ABSTRACT

Electroacupuncture (EA) is an effective alternative for the treatment of functional dyspepsia (FD). It reduces low-grade duodenal inflammation and improves the symptoms of FD by down-regulating the expression of NF-κB p65 and NLRP3, but its mechanism needs to be elucidated. To examine the regulatory effect of electroacupuncture (EA) on intestinal flora and NF-κB p65/ NLRP3 pyroptosis pathway in FD rats. The FD rat model was established via multi-factor stress intervention for two weeks. The rats were randomly divided into the NC group, model group, NF-kB inhibitor group (NF-κB inhibitor BAY 11–7082 was administered), EA group, and EA + NF-kB inhibitor group. After 14 days of treatment, the rats were sacrificed, and the protein and mRNA levels of NF-κB p65, IκB, and NLRP3 in the duodenum were evaluated by Western blotting assays and real-time fluorescent quantitative PCR. The Illumina MiSeq sequencing platform was used to analyze the V4 region of the 16S rRNA gene of intestinal flora and predict functional genes. The concentration of short-chain fatty acids (SCFAs) in feces was assessed by metabolomics. EA can decrease low-grade duodenal inflammation and promote gastrointestinal motility in FD rats. This effect is mediated by inhibition of the NF-κB p65/NLRP3 pyroptosis pathway, an increase in the alpha and beta diversity of gut microbiota in the duodenum, an increase in the abundance of beneficial bacteria at the phylum and genus levels, and an increase in the content of SCFAs. The protective effect of EA against FD might involve multiple hierarchy and pathways. EA may remodel intestinal flora by inhibiting the NF-κB p65/NLRP3 pyroptosis pathway, thereby improving low-grade duodenal inflammation in FD rats.

---

* Corresponding author.
  *E-mail address:* tanglei125716@126.com (L. Tang).

## 1. Introduction

Functional dyspepsia (FD) is a functional gastrointestinal disorder characterized by dyspeptic symptoms, such as epigastric pain, early satiety, and postprandial fullness. There is no clinical, biochemical, endoscopic, or ultrasound evidence that any known organic disease can explain these symptoms [1]. The global prevalence of FD is about 5–7%. Prokinetic agents and proton pump inhibitors (PPI) are the first-line drugs for the clinical treatment of FD; among these, PPI may be slightly more effective [2,3]. However, current treatment options are limited to relieving chronic symptoms, but none of the available treatments are effective on most FD patients. Also, long-term administration of these drugs may cause serious adverse reactions [4]. Acupuncture is a potentially effective non-pharmacological technique for treating FD and is slowly being accepted worldwide. In previous studies [5,6], we showed that electroacupuncture (EA) at "Zusanli" (ST36) and "Taichong" (LR3) can effectively enhance gastric emptying and small intestinal propulsion rate, reduce low-grade duodenal inflammation, and improve the condition of FD rats, with long-lasting and stable effects. Therefore, in this study, we performed EA at ST36 and LR3 to treat FD model rats with liver stagnation and spleen deficiency.

The duodenal microenvironment involves an imbalance of the local microbial community and host and microbial metabolism [7]. The microbiota of saliva, stomach, and duodenum are altered in patients with FD, and these changes may aggravate the symptoms of FD [8]. The intestinal microflora plays a key role in intestinal motility, and the imbalance of intestinal microflora can lead to intestinal dysfunction in mice [9]. Germ-free mice have increased gastric emptying and intestinal transit time in the absence of the GI microbiota compared to wild-type mice [10].

The NF-κB pro-inflammatory signaling pathway plays a key role in the generation of many pro-inflammatory factors [11]. Under inflammatory conditions, NF-κB p65 is phosphorylated and translocated into the nucleus to promote the transcription of inflammatory markers, and induction of inflammation leading to irreversible damage, which is the key mechanism underlying the regulation of inflammatory diseases [12]. The NF-κB pathway also plays a key role in activating the NLRP3 inflammatory intestinal barrier [13]. The NLRP3 inflammasome plays a key role in the development of gut microbiota. Through pyrolysis, NLRP3 converts pro-IL-1 beta into its active form and facilitates the release of inflammatory cytokines. TNF-α, IL-6, and IL-18 can induce a "cytokine storm", such as changes in the composition of the gut microbiota, leading to a vicious cycle [14]. Therefore, NLRP3 might be an effective target for treating FD.

Low-grade inflammation refers to a condition in which the body experiences elevated levels of inflammatory factors due to prolonged, low-dose stimulation by specific immunogens, but without resulting in tissue damage or loss of function [15]. Low-grade duodenal inflammation in FD patients mainly manifests as increased infiltration of mucosal mast cells and eosinophils [16,17], and the number of duodenal eosinophils increases significantly in FD patients who show early satiety and postprandial satiety. This relationship between the increase in cell count and diet-related symptoms might occur through the duodenogastric reflex, which might contribute to the generation of FD-related symptoms [18]. Some studies have found that low-grade inflammation of the duodenal mucosa is closely related to delayed gastric emptying and the severity of dyspeptic symptoms in FD [19]. Since the gastrointestinal microbiota strongly influences low-grade intestinal inflammation and gastrointestinal motility, we hypothesized that EA might improve the symptoms of FD by remodeling the intestinal flora through inhibiting the NF-κB p65/NLRP3 pathway, reducing the pyroptosis of duodenal epithelial cells, and inhibit low-grade duodenal inflammation. Our findings will clarify new mechanisms provided by EA as a traditional Chinese medicine treatment strategy for FD treatment.

## 2. Materials and methods

### 2.1. Establishment and evaluation of animal models

We obtained SPF-grade male Sprague-Dawley (SD) rats (n = 52; weight: 160–180 g) from the Laboratory Animal Center of China Three Gorges University (license number: SYXK (Hubei) 2017–0061). The study was approved by the Ethics Committee of Laboratory Animal Center, Hubei University of Chinese Medicine (ethical batch number: HUCMS 202104003). The main ingredients of the standard diet for rats were corn, secondary meal, imported fish meal, soybean oil, amino acids, vitamins and minerals. Animal feeding environment: the room temperature was $20 \pm 2\,°C$, the humidity was $50 \pm 10\,\%$, normal day/night cycle, and sterile feed and drinking water were available 24 h. All animals were adaptively fed for seven days before the experiment. The 52 rats initially obtained were divided into the NC group (n = 10, rats were isolated in a quiet environment) and the model group. The FD model was established via multi-factor stress intervention which was treated via tail-clip stimulation (30 min each time, twice a day) + irregular feeding (fasting for one day, 200 g of food for both days) + cold normal saline (2 mL each time, twice a day) for 2 weeks. Two rats were randomly selected and evaluated after 2 weeks, and no organic lesions of gastrointestinal tissue were found in those rats.

### 2.2. Animal grouping and intervention

After the models were evaluated, the remaining 50 rats were randomly divided into the normal control group (NC group), model group, EA group, inhibitor group, and EA + inhibitor group (n = 10). The NC group received no intervention. The model group was established via multi-factor stress intervention. In the EA group, the acupoint location was determined following the description provided in Experimental Acupuncture and Moxibustion [20,21]. The $0.25 \times 25$ mm acupuncture needle was used to directly stimulate "ST36″ at a depth of about 12.5 mm, connected to the continuous wave of Han's acupoint nerve stimulator, with a frequency of 2 Hz and an intensity of 1 mA. The bilateral "LR3" (LR3) was oblique stimulate at a depth of 5 mm, and the needles were retained for 30 min each time, once a day. In the inhibitor group, NF-κB inhibitor BAY 11–7082 was mixed with 20 mg/mL DMSO to form a 0.1 mL solution. The rats were intraperitoneally injected once a day with this solution at a dose of 10 mg/kg. In the EA + inhibitor group, EA

and BAY 11–7082 injection were administered once a day. All interventions in the five groups lasted for 2 weeks.

## 2.3. Organizational preparation

At the end of the intervention period, all rats were weighed after fasting for 24 h, and a nutritional semi-solid paste (5 g carboxymethylcellulose, 8 g milk powder, 4 g white sugar, and 4 g starch dissolved in 125 mL distilled water to prepare 150 g nutritious semisolid paste, 2 mL/100 g) and ink (1 mL/100 g) were administered to the rats by gavage based on their body weight. After gavage for 30 min, the rats were anesthetized via inhalation of isoflurane. Then, their neck was cut, blood was collected from the carotid artery, and the stomach and small intestine were removed. The total weight and the net weight of the stomach were weighed. The total length of the small intestine and the distance of ink propulsion were recorded. The tissues from the antrum and duodenum were collected and cut into small sections ($1 \times 1 \times 0.4$ cm), placed on ice, and then, stored in a refrigerator at $-80\ °C$. The tissues were later fixed with 4 % paraformaldehyde at 4 °C.

## 2.4. Gastrointestinal motility test

The body weight of the rats and the amount of food remaining in the food box were measured at 8 a.m. every morning. Gastric emptying rate = (total weight of the stomach - net weight of the stomach)/total weight of the stomach × 100 %. The whole segment of the small intestine was cut and expanded, and the total length of the small intestine (from the orifice to the ileocecal junction) and the length of ink propulsion were measured. Propulsion rate of the small intestine = length of ink propulsion/total length of the small intestine × 100 %.

## 2.5. Hematoxylin & eosin staining of the duodenum

The paraffin sections of the duodenum were deparaffinized using water. The sections were stained with hematoxylin solution, dehydrated, and stained with eosin solution for 5 min. After dehydration, the sections were sealed and examined under a microscope, and images were captured for further analysis.

## 2.6. Biochemical detection of D-xylose

Urine samples (5 μL) were centrifuged at 3000 rpm for 10 min, and the supernatant was collected, which was analyzed using a D-xylose assay kit to determine the xylose content in urine.

## 2.7. Detection of serological indicators

Blood was collected from the carotid artery, centrifuged at 3000 rpm for 10 min, and the supernatant was collected for analysis. Enzyme-linked immunosorbent assay (ELISA) was performed to assess the levels of pro-inflammatory cytokines (IL-1β and IL-18) and lactate dehydrogenase (LDH) in serum.

## 2.8. TUNEL and Caspase-1 immunofluorescence double-staining experiments

Duodenal epithelial tissues were dehydrated, embedded in paraffin, and deparaffinized. Then, the samples were antigen-repaired by treatment with goat serum, blocking at room temperature for 30 min, treatment with primary antibodies, and incubation at 4 °C overnight. Fluorescent (cy3)-labeled sheep anti-mouse IgG was added to the samples and incubated for 1 h. Next, 100 μL of 20 μg/mL Proteinase K solution was added to each sample and incubated for 20 min at room temperature. Each sample was treated with 100 μL of $1 \times$ Equilibration Buffer, which completely covered the sample area to be tested, and the samples were incubated for 15 min at room temperature. TdT incubation buffer was used for optional positive control reactions. It was prepared by thawing the FITC-12-dUTP Labeling Mix on ice while equilibrating cells. The number of pyroptosis-positive cells was calculated in the same part of the tissue.

## 2.9. Western blotting assay

After the total protein was extracted from the tissues, the protein concentration was determined, the proteins were denatured, gels were prepared, electrophoresis was performed to separate the proteins, and finally, electrotransfer was performed. Then, c-Caspase1 p20 and apoptosis-associated speck-like protein (ASC) were transferred onto the membrane at 200 mA for 70 min; GAPDH, IκBα, p-IκBα, Caspase1, and GSDMD p30 were transferred onto the membrane at 200 mA for 90 min; NF-κB p65 and GSDMD were transferred onto the membrane at 200 mA for 120 min; NLRP3 was transferred onto the membrane at 200 mA for 120 min, and then, at 300 mA for 30 min. Immunoblotting was performed using an ECL chromogenic system.

## 2.10. Real-time fluorescence quantitative PCR

Total RNA was extracted by the Trizol method and reverse transcribed into cDNA. The reaction conditions of real-time PCR were 50 °C for 2 min and 95 °C for 10min. 95 °C for 30 s, 60 °C for 30 s and 40 cycles. Dissolution curves were plotted and final data were

**Table 1**
Primer sequence list.

| Name | Primer | Sequence | Size |
|---|---|---|---|
| Rat GAPDH | Forward | 5'- AGTCTACTGGCGTCTTCACC -3' | 225bp |
| | Reverse | 5'-CCACGATGCCAAAGTTGTCA-3' | |
| Rat Caspase 1 | Forward | 5'-AACTGAACAAAGAAGGTGGCG -3' | 155bp |
| | Reverse | 5'-GCAGATAATGAGGGCAAGACG -3' | |
| Rat ASC | Forward | 5'- TCATTGCCAGGGTCACAAAAG -3' | 164bp |
| | Reverse | 5'- CAAGTTCTTGCAGGTCAGGTT -3' | |
| Rat GSDMD | Forward | 5'- CTTGCCGTACTCCATTCCAT -3' | 196bp |
| | Reverse | 5'-TGGGCTGGTCCTGTAAAATC-3' | |
| Rat P65 | Forward | 5'- GCTGATGGAGTACCCTGAAGC -3' | 141bp |
| | Reverse | 5'- ATGTCCGCAATGGAGGAGAAG -3' | |
| Rat NLRP3 | Forward | 5'- CTGCTGAAGTGGATCGAAGTG -3' | 187bp |
| | Reverse | 5'- TGCAAAAGGAAGAAACCACGT-3' | |
| Rat IKBa | Forward | 5'- ATGGCTACCTGGGCATCGTG -3' | 136bp |
| | Reverse | 5'- TTCAACAGGAGCGAGACCAG -3' | |
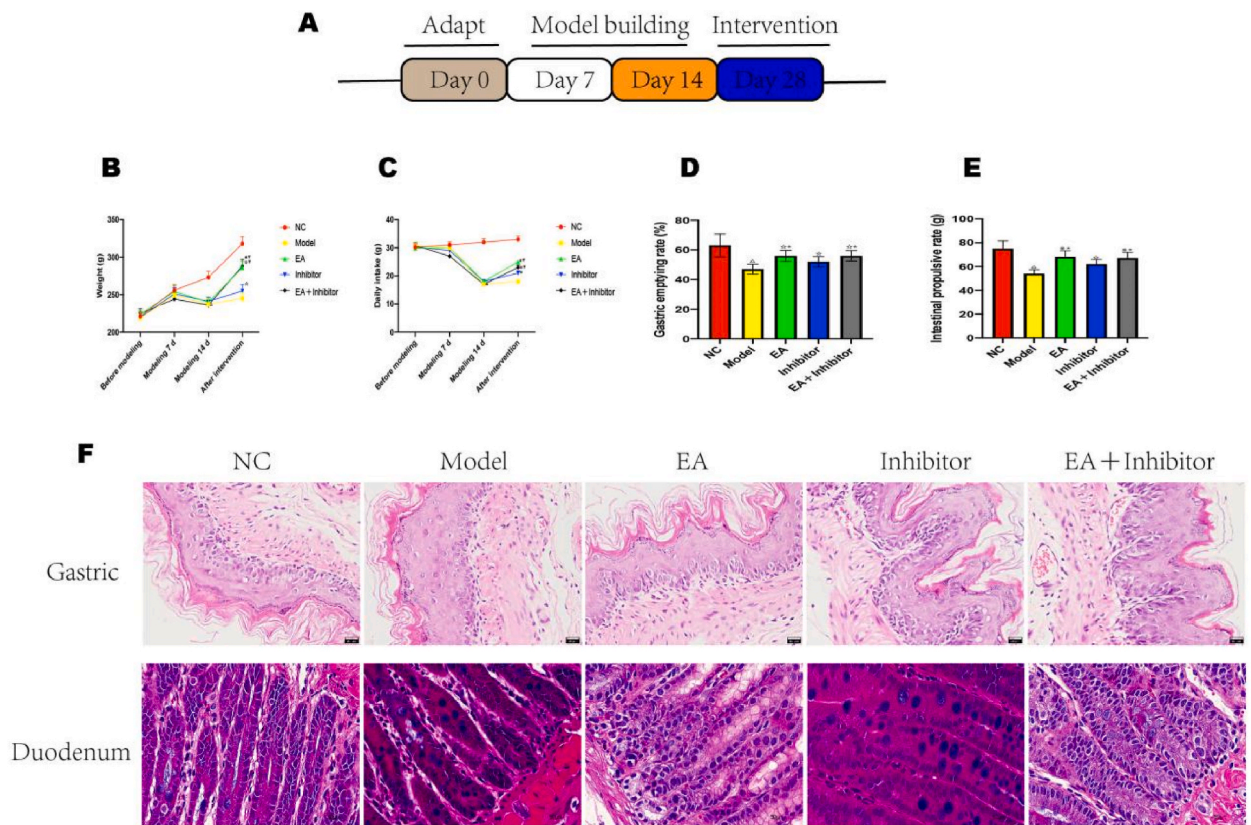


**Fig. 1.** Treatment with EA alleviated the symptoms of FD in rats (n = 8). (A) Experimental flow chart. (B) Body mass of rats (n = 6). (C) Food intake of rats (n = 6). (D) Gastric emptying rate of rats (n = 6). (E) Small bowel propulsion rate (n = 6). (F) Representative images of the duodenum stained with H&E (magnification:400 × ,n = 3). Compared to the NC group: $^{\triangle}P < 0.001$; compared to the model group: $^{*}P < 0.001$ and $^{\star}P < 0.05$; compared to the inhibitor group: $^{\blacktriangledown}P < 0.001$ and $^{\star}P < 0.05$.

analyzed as $2^{-\triangle\triangle Ct}$. The primer sequence list is shown in Table 1.

### 2.11. Sequence analysis of the V4 region of the 16S rRNA gene

After treatment, fresh feces of rats were collected using metabolic cages, and the Illumina MiSeq sequencing platform was used to analyze the V4 region of the 16S rRNA gene of intestinal flora.
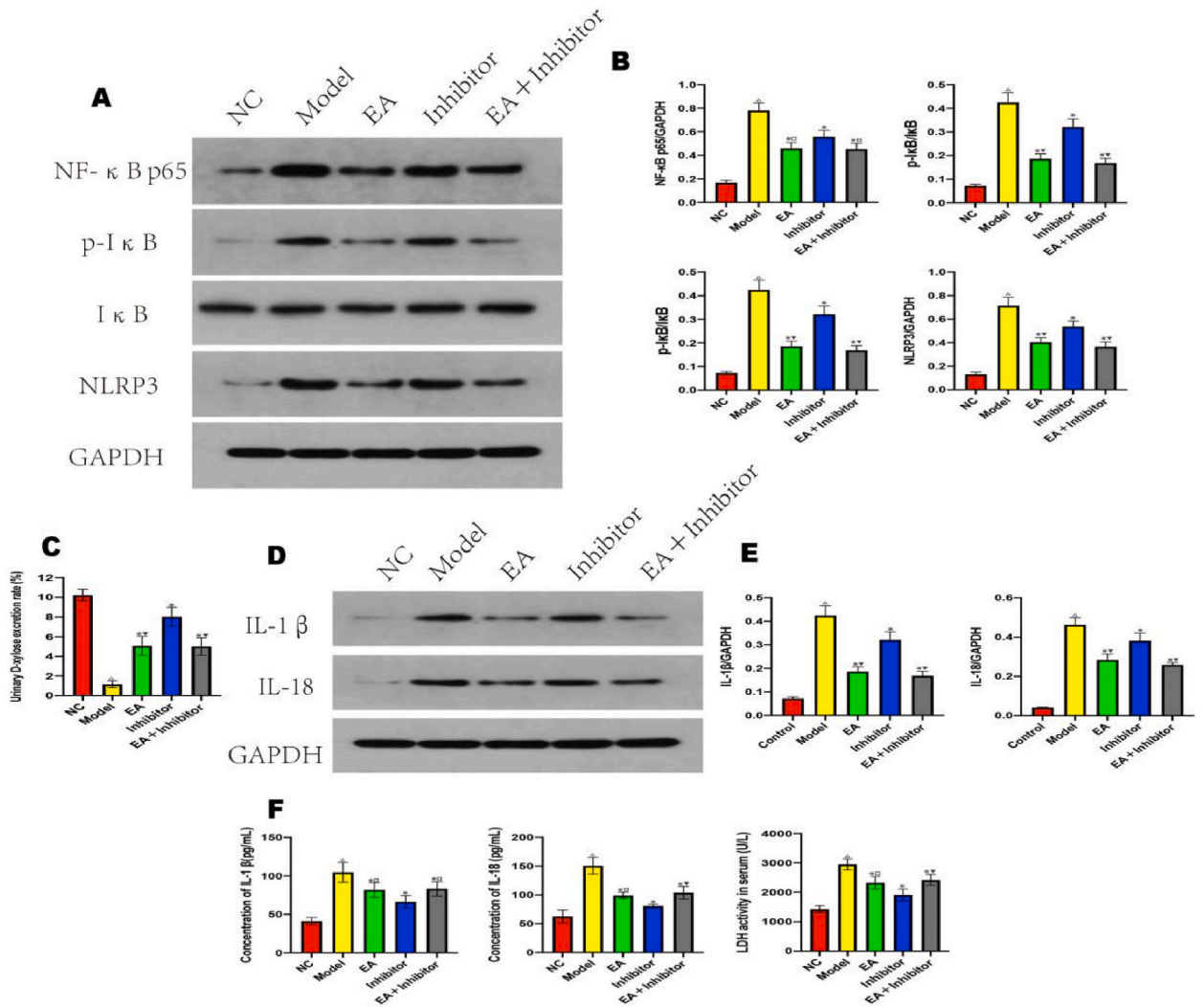
**Fig. 2.** The NF-κB/NLRP3 inflammatory pathway is the key to alleviating FD by EA. (A) Representative Western blots of NF-κB p65, IκB, p-IκB, and NLRP3 (n = 3). (B) Protein semi-quantification of NF-κB p65, IκB, p-IκB, and NLRP3 (n = 3). (C) Urinary D-xylose excretion rate (n = 6). (D) Representative Western blots of IL-1β and IL-18 in the duodenum (n = 3). (E) Semi-quantitative proteins of IL-1β and IL-18 in the duodenum (n = 3). (F) Expression of inflammatory factors IL-1β, IL-18, and LDH in serum (n = 6). Compared to the NC group: $^{\triangle}P < 0.001$; compared to the model group: $^{\ast}P < 0.001$; compared to the inhibitor group: $^{\blacktriangledown}P < 0.001$, $\square P < 0.01$.

### 2.12. Targeted metabolomics

After treatment, fresh feces of rats were collected using metabolic cages, and the concentration of short-chain fatty acids (SCFAs) was evaluated by metabolomics.

### 2.13. Statistical analysis

The SPSS 22.0 statistical software was used for data processing, and all data were expressed as the mean ± SD. After testing for normality and homogeneity, the data were evaluated to determine differences among and between groups by one-way analysis of variance (ANOVA), followed by the Least Significant Difference (LSD) test. Significant p-values associated with microbial clades identified by LEfSe were tested for multiple hypotheses using the Benjamini-Hochberg false discovery rate (FDR) method. Significant p-values for microbial function were determined by STAMP via one-way ANOVA and Tukey's post hoc test. All results were considered to be statistically significant at P < 0.05. Dunnett's multiple comparison test was performed, and graphs were plotted using the GraphPad Prism 9.0 software.
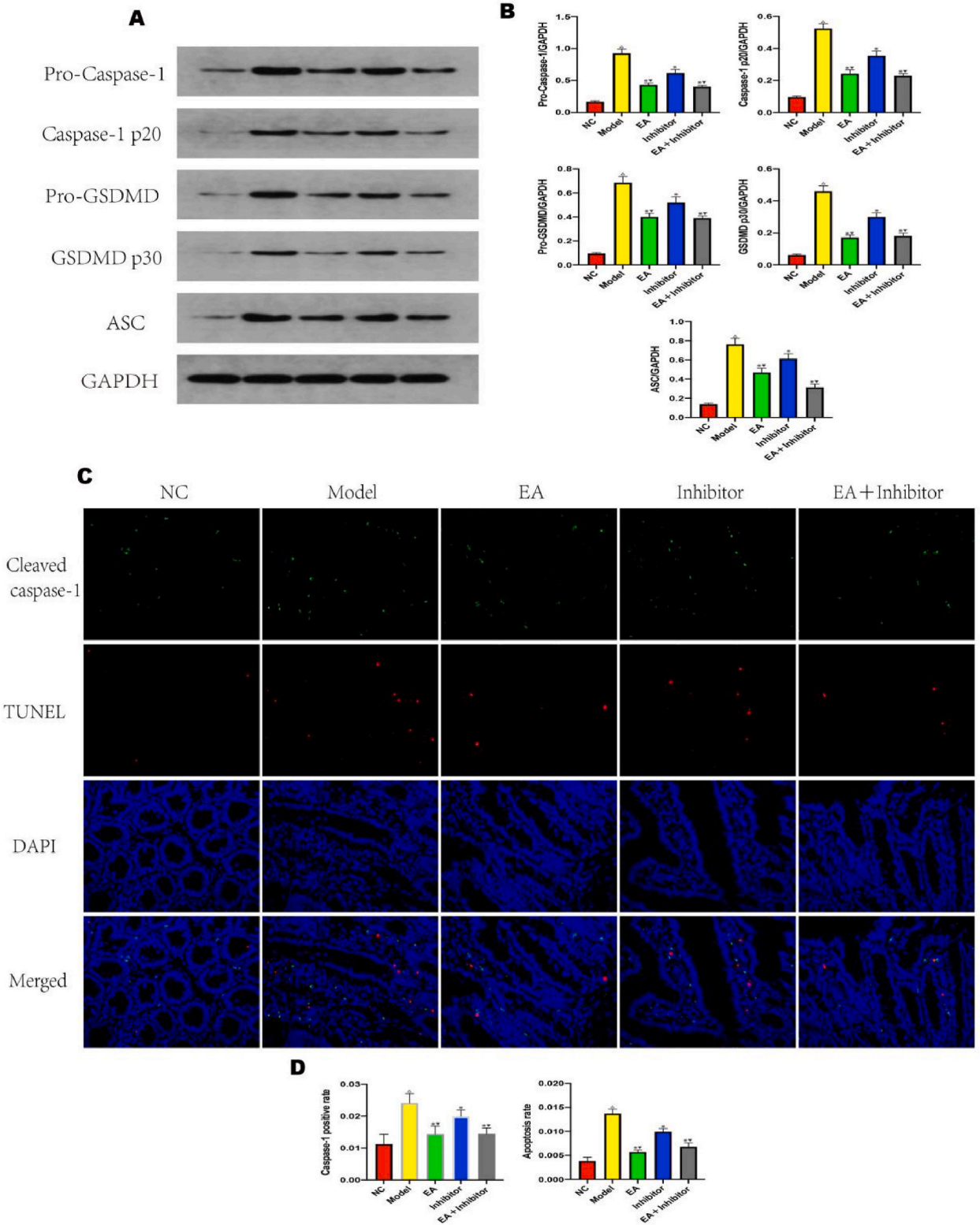
*(caption on next page)*

**Fig. 3.** EA promoted pyroptosis in duodenal epithelial cells of FD rats via the NF-κB/NLRP3 pathway. (A) Representative Western blots of Pro-Caspase-1, Caspase-1 p20, Pro-GSDMD, GSDMD p30, and ASC (n = 3). (B) Protein semi-quantification of Pro-Caspase-1, Caspase-1 p20, Pro-GSDMD, GSDMD p30, and ASC (n = 3). (C) TUNEL and Caspase-1 immunofluorescence double-staining assays were performed (magnification:400, n = 4). (D) The apoptosis rate and Caspase-1-positive rate in duodenal epithelial cells. Compared to the NC group: $^{\triangle}P < 0.001$; compared to the model group: $^{※}P < 0.001$; compared to the inhibitor group: $^{▼}P < 0.001$.

## 3. Results

### 3.1. Electroacupuncture (EA) improved the symptoms of FD in FD rats

To determine the effect of EA on FD, the body weight and food intake of the rats were recorded seven days after adaptive feeding (before modeling), seven days and 14 days after modeling, and 14 days after intervention. The body weight and food intake of the rats in the EA intervention group were significantly higher than those of the rats in the model group (Fig. 1-B and 1-C). The gastric emptying rate and small intestinal propulsion rate of the FD rats in the EA intervention group were also significantly better (Fig. 1-D and 1-E). These results indicated that EA had a beneficial effect on the FD rats. The results of H&E staining (Fig. 1-F) showed that no pathological changes, such as ulcers and bleeding, occurred in the intestinal mucosa of gastric and duodenal tissues in the rats of any group, which confirms that the FD rat model has been successfully established.

### 3.2. The NF-κB/NLRP3 inflammatory pathway is the key to treating FD by EA

As the NF-κB/NLRP3 pathway plays an important role in regulating the development of intestinal inflammation, we evaluated whether the NF-κB/NLRP3 pathway plays a key role in the treatment of FD. We inhibited the NF-κB/NLRP3 pathway with the inhibitor BAY 11–7082, and treated rats with EA and the inhibitor for two weeks. We found that EA significantly increased the expression of NF-κB p65, p-IκB, and NLRP3 proteins in the duodenum of FD rats (Fig. 2-A and 2-B) and decreased the expression of IL-1β and IL-18 proteins in the duodenum (Fig. 2-D and 2-E). However, no additive effect was found between the inhibitor group and the EA + inhibitor group. The concentration of D-xylose can indirectly reflect the severity of the qi deficiency syndrome and the recovery after treatment [20]. EA also increased the rate of urinary D-xylose excretion (Fig. 2-C) and decreased serum levels of IL-1β, IL-18, and LDH (Fig. 2-F) in FD rats. These results confirmed that EA can reduce low-grade duodenal inflammation in FD rats through the NF-κB/NLRP3 inflammatory pathway.

### 3.3. EA promoted the pyroptosis of duodenal epithelial cells

Based on the changes in the NF-κB/NLRP3 pathway, we confirmed that EA significantly upregulated the expression of pyroptosis-related proteins Pro-Caspase-1, Caspase-1 p20, Pro-GSDMD, the N-terminal active component p30 of GSDMD (GSDMD p30), and ASC in the duodenum of FD rats (Fig. 3-A and 3-B). The results of TUNEL and Caspase-1 immunofluorescence double-staining assays confirmed that EA decreased the rate of pyroptosis in duodenal epithelial cells (Fig. 3-C and 3-D). However, no additive effect was found between the inhibitor group and the EA + inhibitor group.

### 3.4. EA regulated the remodeling of duodenal flora

We found that EA alleviated low-grade intestinal inflammation by regulating the duodenal microbiota. EA significantly increased the Chao1 index and Simpson index of alpha diversity. The beta diversity indicated that the spatial distance between the EA group and the NC group was small (Fig. 4-A). In the beta diversity analysis, the EA group and the EA + inhibitor group were more similar in the structure of the duodenal flora, which was significantly different from the duodenal flora of the rats in the model group and the inhibitor group, and similar to the duodenal flora of the rats in the NC group (Fig. 4-B). The top four most abundant phyla were Firmicutes, Bacteroidetes, Actinobacteria, and Proteobacteria. The three most abundant genera were *Lactobacillus, Prevotella, and Blautia*. EA increased the relative abundance of Firmicutes and decreased the abundance of Bacteroidetes (Fig. 4-C); it also increased the abundance of *Lactobacillus* (Fig. 4-D). These results suggested that EA may regulate the composition of the intestinal flora and reduce low-grade inflammation by increasing the abundance of beneficial bacteria and decreasing the abundance of pathogenic bacteria.

We found 34 different species with an LDA scor e > 2, and the NC group had the most prominent effect on Clostridia (LDA score >3) (Fig. 5-A and 5-B). The influence of the model group on the genus p_75_a5 was the most prominent (LDA score >3). The effect of EA on Actinobacteria was the most prominent (LDA score >4). The inhibitor had the strongest effect on Pseudomonadaceae (LDA score >3). The effect of EA + inhibitor on *Shigella* was the most prominent (LDA score >3).

Although the results of the detection of gut microbiota in FD rats showed that the site of action of EA is the gut, the possibility that EA affects other functional pathways cannot be excluded. The function prediction of gut microbiota samples in this study was mainly related to metabolic pathways. The secondary functional pathways related to metabolic pathway were associated with carbohydrate metabolism (relative abundance 5374.12), metabolism of cofactors and vitamins (relative abundance 3859.36), and amino acid metabolism (relative abundance 3457.75) (Fig. 5-C).
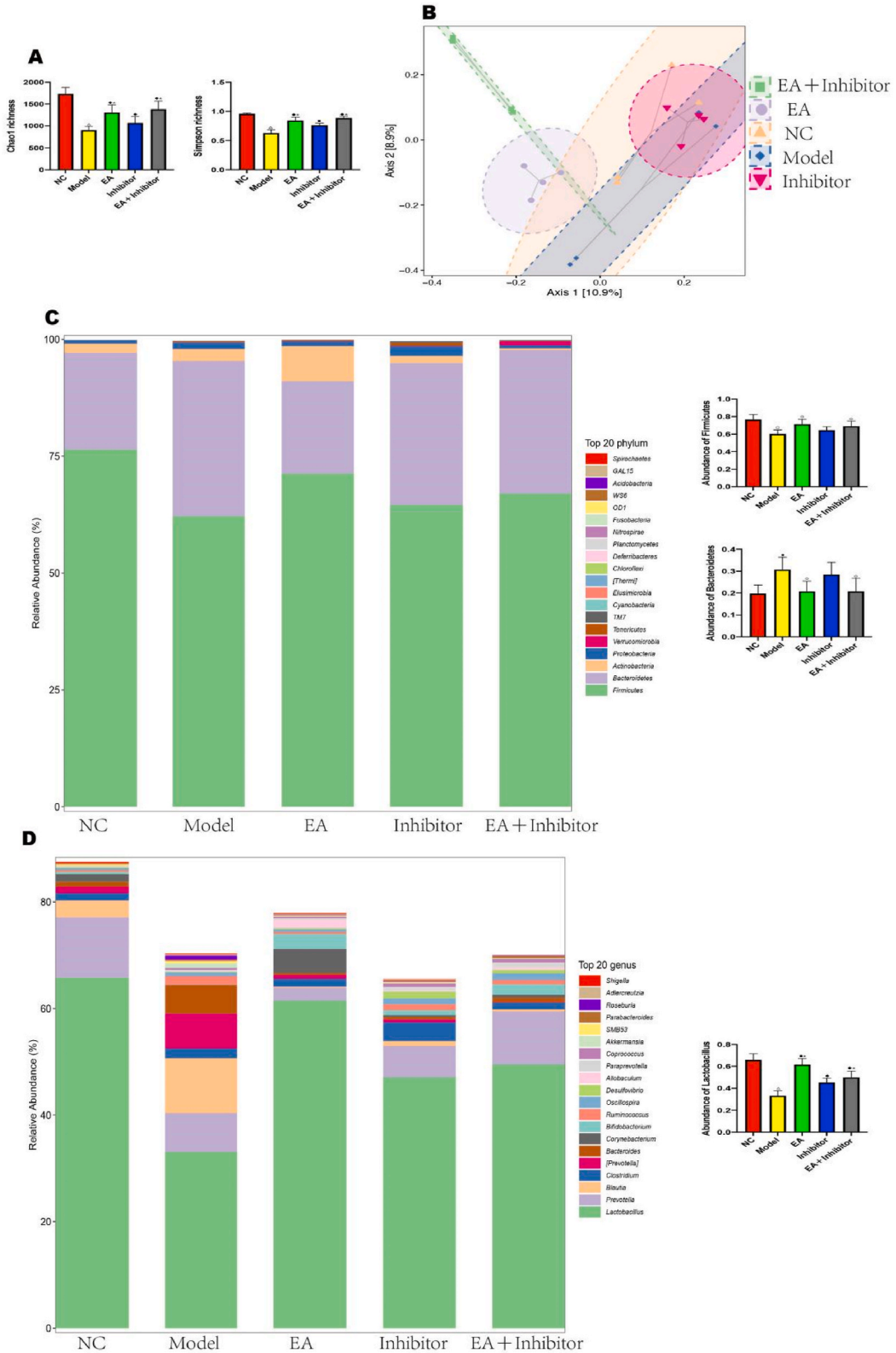
*(caption on next page)*

**Fig. 4.** Remodeling of the duodenal gut microbiota by EA. (A) Alpha diversity of gut microbiota (n = 4). (B) Beta diversity analysis of gut microbiota (n = 4). (C) Comparison of the relative abundance of intestinal flora at the phylum level and changes in the abundance of Firmicutes and Bacteroidetes (n = 4). (D) Comparison of the relative abundance of gut microbiota at the genus level and changes in the abundance of *Lactobacillus* (n = 4). Compared to the NC group: $^\triangle P < 0.001$, $^\circ P < 0.01$, and $^\bullet P < 0.05$; compared to the model group: $^\blacksquare P < 0.001$, $^\blacklozenge P < 0.01$, and $^\circ P < 0.05$; compared to the inhibitor group: $^\star P < 0.05$.

*3.5. EA increased the expression of SCFAs*

Short-chain fatty acids (SCFAs) regulate various activities in the GI tract, including cell proliferation and differentiation, water and electrolyte absorption, hormone secretion, and immune system activation [22]. We found that EA significantly increased acetic acid, propionic acid, isobutyric acid, butyric acid, isovaleric acid, valeric acid, and caproic acid in the feces of FD rats. The concentration of SCFAs is shown in Fig. 6 A-G. However, no additive effect was found between the inhibitor group and the EA + inhibitor group.

**4. Discussion**

Many pathophysiological studies on FD have investigated gastrointestinal motility. Researchers investigating duodenal mucosal changes in FD have shifted their focus from motor to low-grade inflammation, including duodenal mucosal permeability and eosinophil infiltration. Several studies have found that EA has beneficial effects on the gastrointestinal motility of individuals with FD [23]. We found that EA increased the gastric emptying rate and the small intestinal propulsion rate in FD model rats established by multi-factor stress intervention. These findings indicated that EA effectively promoted gastrointestinal motility (Fig. 1).

The NF-κB p65/NLRP3 signaling pathway is an important inflammatory pathway, which is involved in the regulation of duodenal permeability and inflammation [24]. One function of p–NF–κB is to activate the NLRP3 inflammasome [25]. Activation of the NF-κB p65/NLRP3 signaling pathway within macrophages stimulates the production of proinflammatory cytokines such as IL-1β, IL-6, and TNF-α [26]. In the atypical pathway, reactive oxygen species (ROS) activate the NLRP3 inflammasome by activating caspase-1 [27–29]. Activation of the NLRP3 inflammasome, in turn, activates caspase-1, which converts IL-1β and IL-18 to mature IL-1β and IL-18 [30], cleaving the N-terminal sequence of Gasdermin D (GSDMD). This sequence binds to the membrane and creates a membrane pore, which leads to pyroptosis. Thus, GSDMD plays a key role in the activation of pyroptosis [31,32]. Complexes such as NLRP3, ASC, and caspase-1 induce cleavage of IL-1β from the precursor of IL-1β [33,34]. Therefore, the NF-κB p65/NLRP3 pyroptosis pathway was targeted as a potential strategy to reduce low-grade duodenal inflammation. Our findings confirmed that EA promoted the pyroptosis of duodenal epithelial cells through the NF-κB/NLRP3 pathway and decreased low-grade duodenal inflammation in FD rats, but no additive effect was found between the inhibitor group and the EA + inhibitor group (Figs. 2 and 3).

The duodenal microenvironment is an important factor in the pathophysiological mechanism of FD [35]. Several researchers have shown that acupuncture affects the metabolism and function of the host by regulating the intestinal flora [36,37]. Psychological stress disrupts the integrity of the duodenal barrier, leading to an increase in permeability and low-grade inflammation and alterations in duodenal contents, including bile acids, lipids, and microbiota. Thus, psychological stress might play an important role in stimulating low-grade inflammation [38–40]. Intestinal motility is affected by various factors, including the nervous and immune systems, mucus secretion, gastrointestinal microbiota, and fermentation products [41]. Some studies have shown that the imbalance of intestinal flora can lead to abnormal intestinal functions and decrease the diversity of intestinal microbial flora in mice [41]. Additionally, the release of a large number of pathogenic bacteria can increase the endotoxin in the human gut and destroy the intestinal mucosal barrier, leading to intestinal dysfunction [42]. Our results showed that EA significantly increased the alpha diversity and beta diversity in the duodenum, increased the abundance of Firmicutes, decreased the abundance of Bacteroidetes, and increased the abundance of *Lactobacillus* (Fig. 4). These changes suggested that EA can regulate the composition of the intestinal flora by increasing the abundance of beneficial bacteria and decreasing the abundance of pathogenic bacteria; the alteration of the microbial community, in turn, can reduce low-grade inflammation of the duodenum.

Short-chain fatty acids (SCFAs) are the most common metabolites of the intestinal flora. The main SCFAs identified were acetic acid, propionic acid, and butyric acid, whereas the proportion of formic acid, valeric acid, and caproic acid was relatively small [43]. Acetic acid and propionic acid are mainly produced by Firmicutes and *Bacteroides*, which were the most prevalent bacteria and constituted 80–90 % of the gut microbiota [44,45]. Some studies have shown that SCFAs can act as a food substrate for colonic bacteria. They can also regulate leukocyte function and activate the immune system by facilitating the production of different eicosanesulfonic acids and cytokines (IL-2, IL-6, IL-10, and TNF-α), promote the production of chemokines, and induce a balance between pro-inflammatory and anti-inflammatory mechanisms [46]. SCFAs can also regulate the intestinal barrier and reduce the pH of the intestine, which favors the growth of probiotics but inhibits the growth and colonization of pathogenic bacteria, such as *Escherichia coli* and *Shigella* [47]. We found that EA increased the level of SCFAs in FD rats and the abundance of Firmicutes and *Lactobacillus* in the intestine, but it decreased the abundance of Bacteroidetes.

Our studies present several limitations. First, only male rats were used in this study. A dedicated study was needed to account for potential sex variability. Second, the direct mechanism by which EA reduces low-grade inflammation in the duodenum through gut microbiota was not determined because this study was conducted without determination of the inflammation effects after interrupting intestinal flora.

In short, EA can decrease low-grade duodenal inflammation and promote gastrointestinal motility in FD rats. This effect is mediated by inhibition of the NF-κB p65/NLRP3 pyroptosis pathway, an increase in the alpha and beta diversity of gut microbiota in the
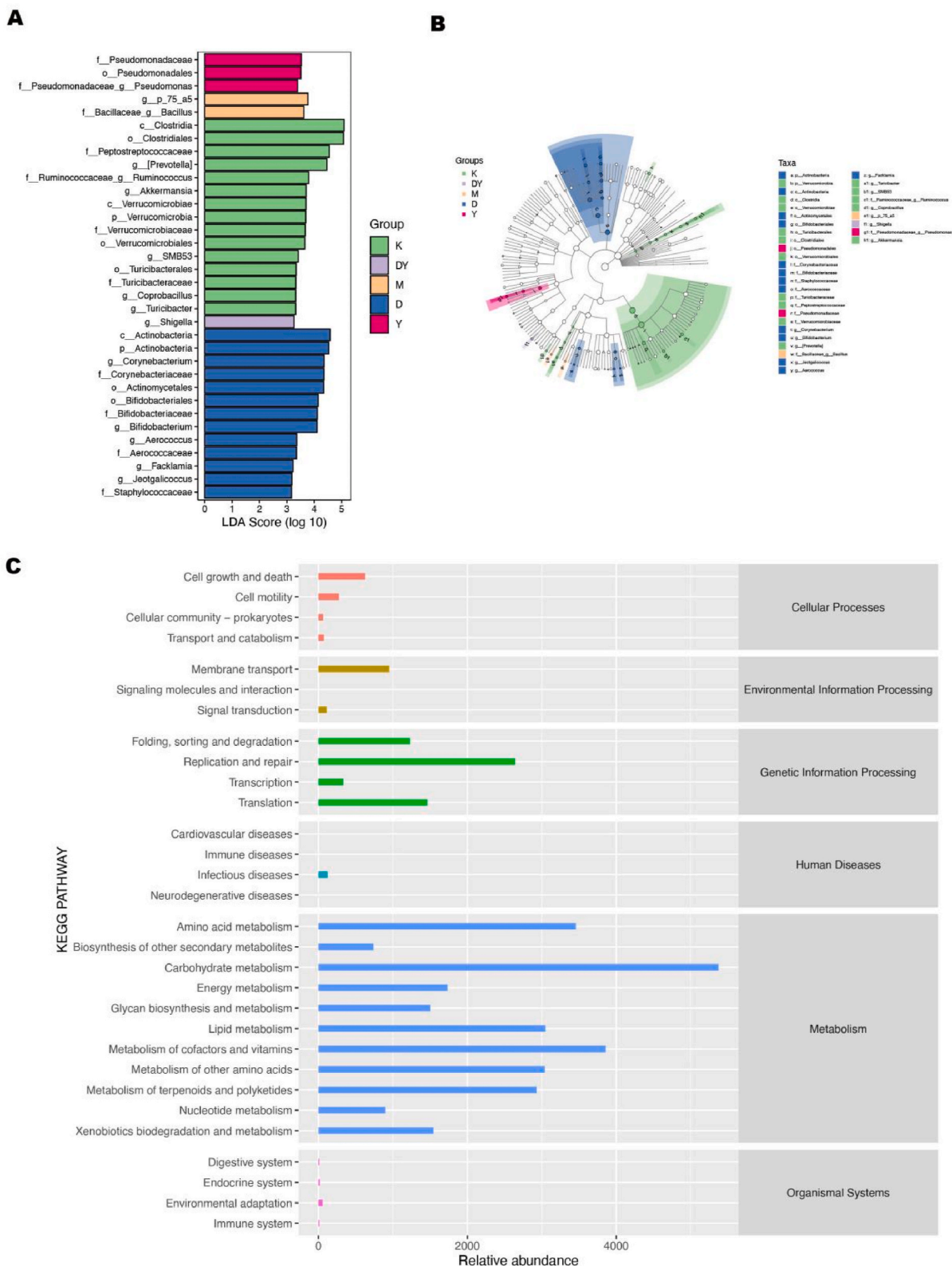
**Fig. 5.** Remodeling of the duodenal gut microbiota by EA. (A) A bar graph of the LDA effect values for the marker species. (B) The differences between taxonomic groups were determined based on the classification hierarchy tree. (C) The predicted abundance map of the KEGG secondary functional pathways.
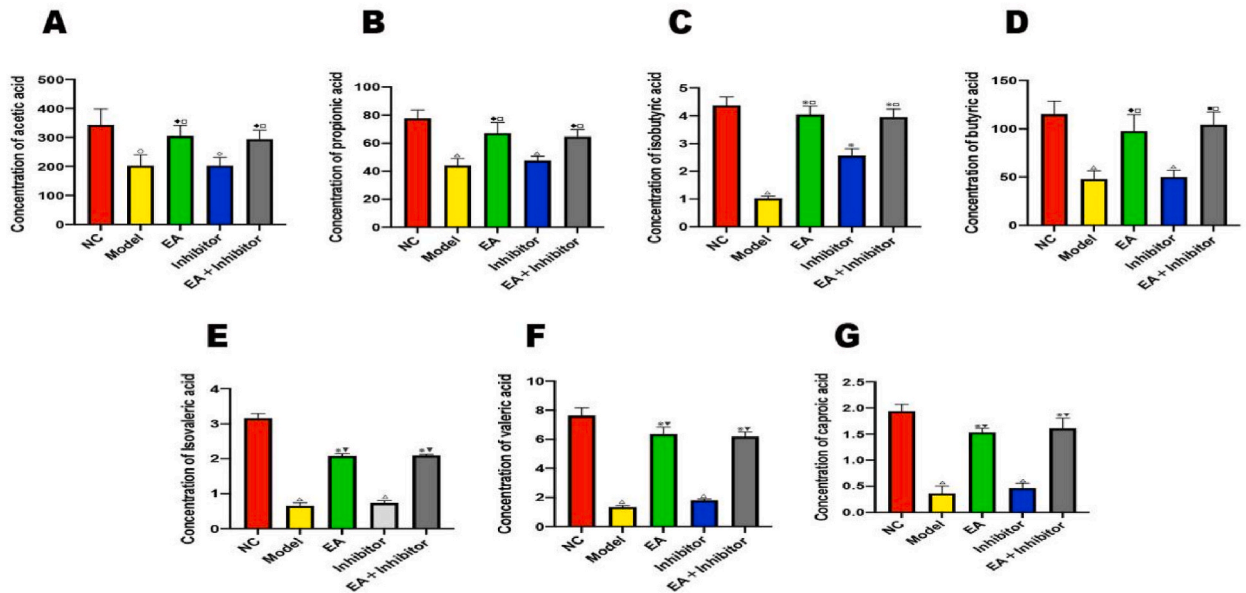
**Fig. 6.** Benign regulation of fecal SCFAs in rats by EA. The concentrations of acetic acid (A), propionic acid (B), isobutyric acid (C), butyric acid (D), isovaleric acid (E), valeric acid (F), and caproic acid were evaluated in the feces of rats in all groups (n = 4). Compared to the NC group: $^{\triangle}P < 0.001$; compared to the model group: $^{*}P < 0.001$, and $^{\blacklozenge}P < 0.01$; compared to the inhibitor group: $^{\blacktriangledown}P < 0.001$ and $^{\square}P < 0.01$.

duodenum, an increase in the abundance of beneficial bacteria at the phylum and genus levels, and an increase in the content of SCFAs. The protective effect of EA against FD might involve multiple hierarchy and pathways. The use of probiotics as an additional treatment for several immunocorrelated and autoimmune diseases that may cause dyspepsia [48], we will further explore the therapeutic effect of the combined intervention of EA and probiotics on FD.

### Ethics statement

The study was approved by the Ethics Committee of Laboratory Animal Center, Hubei University of Chinese Medicine (ethical batch number: HUCMS 202104003).

### Funding statement

### Data availability statement

Data will be made available on request.

### Additional information

No additional information is available for this paper.

### CRediT authorship contribution statement

**Yong-Li Han:** Writing – review & editing, Writing – original draft, Project administration, Data curation. **Zhao-Xia Kang:** Project administration, Funding acquisition. **Shu-Wen Jin:** Project administration. **Xiao-Li Pan:** Project administration. **Hong-Xing Zhang:** Validation, Supervision, Data curation. **Liang-Yu Zhang:** Validation, Supervision. **Lei Tang:** Validation, Supervision.

### Declaration of competing interest

The authors declare that they have no known competing financial interests or personal relationships that could have appeared to influence the work reported in this paper.

# Appendix A. Supplementary data

Supplementary data to this article can be found online at https://doi.org/10.1016/j.heliyon.2024.e31197.

# References

[1] A.C. Ford, S. Mahadeva, M.F. Carbone, B.E. Lacy, N.J. Talley, Functional dyspepsia, Lancet 8 (4) (2020) 1689–1702, https://doi.org/10.1016/S0140-6736(20)30469-4.

[2] T. Tomita, T. Oshima, H. Miwa, New approaches to diagnosis and treatment of functional dyspepsia, Curr. Gastroenterol. Rep. 20 (12) (2018) 55, https://doi.org/10.1007/s11894-018-0663-4.

[3] B.E. Lacy, R.C. Chase, D.J. Cangemi, The treatment of functional dyspepsia: present and future, Expet Rev. Gastroenterol. Hepatol. 17 (1) (2023) 9–20, https://doi.org/10.1080/17474124.2023.2162877.

[4] I. Masuy, L. Van Oudenhove, J. Tack, Review article: treatment options for functional dyspepsia, Aliment. Pharmacol. Ther. 49 (9) (2019) 1134–1172, https://doi.org/10.1111/apt.15191.

[5] Dan Wang, Hong-xing Zhang, Pei-jing Rong, Li-wei Hou, Shao-yuan Li, Yu Wang, Jun-ying Wang, Jin-ling Zhang, Bin Zhao, Xiao Guo, Yue Zhang, Zi-xuan Zhang, Yi-fei Wang, Jia-kai He, Yong-li Han, Effect of electroacupuncture on duodenal mucosal barrier and its regutey protcin in rats of functional dyspepsia with liver stagnation and spleen deficiency, J. Basic Chin. Med. 12 (2020) 1843–1845+1882, https://doi.org/10.19945/j.cnki.issn.1006-3250.2020.12.028.

[6] D. Wang, J. Zhang, D. Yang, J. Wang, J.L. Li, Y. Han, Z. Kang, H. Zhang, Electroacupuncture restores intestinal mucosal barrier through TLR4/NF-κB p65 pathway in functional dyspepsia-like rats, Anat. Rec. 306 (12) (2021) 2927–2938, https://doi.org/10.1002/ar.24800.

[7] L. Wauters, N.J. Talley, M.M. Walker, J. Tack, T. Vanuytsel, Novel concepts in the pathophysiology and treatment of functional dyspepsia, Gut 69 (3) (2020) 591–600, https://doi.org/10.1136/gutjnl-2019-318536.

[8] J. Cervantes, M. Michael, B.Y. Hong, A. Springer, H. Guo, B. Mendoza, M. Zeng, O. Sundin, R. McCallum, Investigation of oral, gastric, and duodenal microbiota in patients with upper gastrointestinal symptoms, J. Invest. Med. (2020), https://doi.org/10.1136/jim-2020-001642 jim-2020-001642.

[9] R. Fu, Z. Li, R. Zhou, C. Li, S. Shao, J. Li, The mechanism of intestinal flora dysregulation mediated by intestinal bacterial biofilm to induce constipation, Bioengineered 12 (1) (2021) 6484–6498, https://doi.org/10.1080/21655979.2021.1973356.

[10] X. Bai, G. De Palma, E. Boschetti, Y. Nishiharo, J. Lu, C. Shimbori, A. Costanzini, Z. Saqib, N. Kraimi, S. Sidani, S. Hapfelmeier, A.J. Macpherson, E.F. Verdu, R. De Giorgio, S.M. Collins, P. Bercik, Vasoactive intestinal polypeptide plays a key role in the microbial-neuroimmune control of intestinal motility, Cell Mol Gastroenterol Hepatol 17 (3) (2024) 383–398, https://doi.org/10.1016/j.jcmgh.2023.11.012.

[11] B. Hoesel, J.A. Schmid, The complexity of NF-κB signaling in inflammation and cancer, Mol. Cancer 12 (2013) 86, https://doi.org/10.1186/1476-4598-12-86.

[12] X. Deng, Y. Wang, L. Tian, M. Yang, S. He, Y. Liu, A. Khan, Y. Li, J. Cao, G. Cheng, Anneslea fragrans wall ameliorates ulcerative colitis via inhibiting NF-κB and MAPK activation and mediating intestinal barrier integrity, J. Ethnopharmacol. 278 (2021) 114304, https://doi.org/10.1016/j.jep.2021.114304.

[13] L. Ge, Z. Lin, G. Le, L. Hou, X. Mao, S. Liu, D. Liu, F. Gan, K. Huang, Nontoxic-dose deoxynivalenolaggravates lipopolysaccharides-induced inflammation and tight junction disorder in IPEC-J2 cells through activation of NF-κB and LC3B, Food Chem. Toxicol. 145 (2020) 111712, https://doi.org/10.1016/j.fct.2020.111712.

[14] G. Marano, M. Mazza, F.M. Lisci, M. Ciliberto, G. Traversi, G.D. Kotzalidis, D. De Berardis, L. Laterza, G. Sani, A. Gasbarrini, E. Gaetani, The microbiota-gut-brain Axis: psychoneuroimmunological insights, Nutrients 15 (6) (2023) 1496, https://doi.org/10.3390/nu15061496.

[15] M. Tristan Asensi, A. Napoletano, F. Sofi, M. Dinu, Low-grade inflammation and ultra-processed foods consumption: a review, Nutrients 15 (6) (2023) 1546, https://doi.org/10.3390/nu15061546.

[16] S. Safiri, E. Ayubi, Letter: functional dyspepsia is associated with duodenal eosinophilia in an Australian paediatric cohort-methodological issues to avoid misinterpretation, Aliment. Pharmacol. Ther. 46 (3) (2017) 387, https://doi.org/10.1111/apt.14158.

[17] H. Vanheel, M. Vicario, T. Vanuytsel, L. Van Oudenhove, C. Martinez, Å.V. Keita, N. Pardon, J. Santos, J.D. Söderholm, J. Tack, R. Farré, Impaired duodenal mucosal integrity and low-grade inflammation in functional dyspepsia, Gut 63 (2) (2014) 262–271, https://doi.org/10.1136/gutjnl-2012-303857.

[18] B. Nojkov, S.Y. Zhou, R.D. Dolan, E.M. Davis, H.D. Appelman, X. Guo, K. Jackson, M.B. Sturm, T.D. Wang, C. Owyang, J.J. Liu, W.D. Chey, Evidence of duodenal epithelial barrier impairment and increased pyroptosis in patients with functional dyspepsia on confocal laser endomicroscopy and "ex vivo" mucosa analysis, Am. J. Gastroenterol. 115 (11) (2020) 1891–1901, https://doi.org/10.14309/ajg.0000000000000827.

[19] K. Elkholey, M. Niewiadomska, L. Morris, S. Whyte, J. Houser, M.B. Humphrey, S. Stavrakis, Transcutaneous vagus nerve stimulation ameliorates the phenotype of heart failure with preserved ejection fraction through its anti-inflammatory effects, Circ Heart Fail 15 (8) (2022) e009288, https://doi.org/10.1161/CIRCHEARTFAILURE.122.009288.

[20] D.S. Xu, S. Zhao, J.J. Cui, T.M. Ma, B. Xu, X.C. Yu, B. Zhu, X.H. Jing, W.Z. Bai, A new attempt of re-mapping acupoint atlas in the rat, Zhen Ci Yan Jiu 44 (1) (2019) 62–65, https://doi.org/10.13702/j.1000-0607.180396. Chinese.

[21] Ming Zhang, Jing Wu, Zhen Peng, Ronghua Cui, Jinghua Zhang, Xixiong Xiang, Effect of heze granules on GAS,D-xylose and CK in rats with spleen deficiency, J. Emergency in Traditional Chin. 29 (2) (2020) 267–269+277, https://doi.org/10.3969/j.issn.1004-745X.2020.02.021.

[22] X. Xie, C. Geng, X. Li, J. Liao, Y. Li, Y. Guo, C. Wang, Roles of gastrointestinal polypeptides in intestinal barrier regulation, Peptides 151 (2022) 170753, https://doi.org/10.1016/j.peptides.2022.170753.

[23] T. Oshima, Functional dyspepsia: current understanding and future perspective, Digestion 105 (1) (2024) 26–33, https://doi.org/10.1159/000532082.

[24] M. Camilleri, T. Zheng, Cannabinoids and the gastrointestinal tract, Clin. Gastroenterol. Hepatol. 21 (13) (2023) 3217–3229, https://doi.org/10.1016/j.cgh.2023.07.031.

[25] J. Zeng, Y. Chen, R. Ding, L. Feng, Z. Fu, S. Yang, X. Deng, Z. Xie, S. Zheng, Isoliquiritigenin alleviates early brain injury after experimental intracerebral hemorrhage via suppressing ROS- and/or NF-κB-mediated NLRP3 inflammasome activation by promoting Nrf2 antioxidant pathway, J. Neuroinflammation 14 (1) (2017) 119, https://doi.org/10.1186/s12974-017-0895-5.

[26] Y. He, Z. Li, T. Xu, D. Luo, Q. Chi, Y. Zhang, S. Li, Polystyrene nanoplastics deteriorate LPS-modulated duodenal permeability and inflammation in mice via ROS drived-NF-κB/NLRP3 pathway, Chemosphere 307 (Pt 1) (2022) 135662, https://doi.org/10.1016/j.chemosphere.2022.135662.

[27] M. Qoreishi, M. Panahi, O. Dorodi, N. Ghanbari, S.S. Jousheghan, Involvement of NF-κB/NLRP3 axis in the progression of aseptic loosening of total joint arthroplasties: a review of molecular mechanisms, Naunyn-Schmiedeberg's Arch. Pharmacol. 395 (7) (2022) 757–767, https://doi.org/10.1007/s00210-022-02232-4.

[28] J.F. Teng, Q.B. Mei, X.G. Zhou, Y. Tang, R. Xiong, W.Q. Qiu, R. Pan, B.Y. Law, V.K. Wong, C.L. Yu, H.A. Long, X.L. Xiao, F. Zhang, J.M. Wu, D.L. Qin, A.G. Wu, Polyphyllin VI induces caspase-1-mediated pyroptosis via the induction of ROS/NF-κB/NLRP3/GSDMD signal Axis in non-small cell lung cancer, Cancers 12 (1) (2020) 193, https://doi.org/10.3390/cancers12010193.

[29] F. Wang, Q. Liang, Y. Ma, M. Sun, T. Li, L. Lin, Z. Sun, J. Duan, Silica nanoparticles induce pyroptosis and cardiac hypertrophy via ROS/NLRP3/Caspase-1 pathway, Free Radic. Biol. Med. 182 (2022) 171–181, https://doi.org/10.1016/j.freeradbiomed.2022.02.027.

[30] X. Jiang, C. Ma, Y. Gao, H. Cui, Y. Zheng, J. Li, W. Zong, Q. Zhang, Tongxinluo attenuates atherosclerosis by inhibiting ROS/NLRP3/caspase-1-mediated endothelial cell pyroptosis, J. Ethnopharmacol. 304 (2023) 116011, https://doi.org/10.1016/j.jep.2022.116011.

[31] T. Sho, J. Xu, Role and mechanism of ROS scavengers in alleviating NLRP3-mediated inflammation, Biotechnol. Appl. Biochem. 66 (1) (2019) 4–13, https://doi.org/10.1002/bab.1700.

[32] Y. Wang, X. Zhu, S. Yuan, S. Wen, X. Liu, C. Wang, Z. Qu, J. Li, H. Liu, L. Sun, F. Liu, TLR4/NF-κB signaling induces GSDMD-related pyroptosis in tubular cells in diabetic kidney disease, Front. Endocrinol. 10 (2019) 603, https://doi.org/10.3389/fendo.2019.00603.

[33] L. Sun, W. Ma, W. Gao, Y. Xing, L. Chen, Z. Xia, Z. Zhang, Z. Dai, Propofol directly induces caspase-1-dependent macrophage pyroptosis through the NLRP3-ASC inflammasome, Cell Death Dis. 10 (8) (2019) 542, https://doi.org/10.1038/s41419-019-1761-1764.

[34] N. Dubchak, G.F. Falasca, New and improved strategies for the treatment of gout, Int. J. Nephrol. Renovascular Dis. 3 (2010) 145–166, https://doi.org/10.2147/IJNRD.S6048.

[35] L. Wauters, N.J. Talley, M.M. Walker, J. Tack, T. Vanuytsel, Novel concepts in the pathophysiology and treatment of functional dyspepsia, Gut 69 (3) (2020) 591–600, https://doi.org/10.1136/gutjnl-2019-318536.

[36] C. Bao, L. Wu, D. Wang, L. Chen, X. Jin, Y. Shi, G. Li, J. Zhang, X. Zeng, J. Chen, H. Liu, H. Wu, Acupuncture improves the symptoms, intestinal microbiota, and inflammation of patients with mild to moderate Crohn's disease: a randomized controlled trial, EClinicalMedicine 45 (2022) 101300, https://doi.org/10.1016/j.eclinm.2022.101300.

[37] W. Feng, Z. Yang, Y. Liu, R. Chen, Z. Song, G. Pan, Y. Zhang, Z. Guo, X. Ding, L. Chen, Y. Wang, Gut microbiota: a new target of traditional Chinese medicine for insomnia, Biomed. Pharmacother. 160 (2023) 114344, https://doi.org/10.1016/j.biopha.2023.114344.

[38] L.R. Zhu, S.S. Li, W.Q. Zheng, W.J. Ni, M. Cai, H.P. Liu, Targeted modulation of gut microbiota by traditional Chinese medicine and natural products for liver disease therapy, Front. Immunol. 14 (2023) 1086078, https://doi.org/10.3389/fimmu.2023.1086078.

[39] K. Fan, N.J. Talley, Functional dyspepsia and duodenal eosinophilia: a new model, J Dig Dis 18 (12) (2017) 667–677, https://doi.org/10.1111/1751-2980.12556.

[40] M. Xu, L. Wang, Y. Guo, W. Zhang, Y. Chen, Y. Li, Corrigendum to "positive effect of electro-acupuncture treatment on gut motility in constipated mice is related to rebalancing the gut microbiota", Evid Based Complement Alternat Med 2021 (2021) 9835654, https://doi.org/10.1155/2021/9835654.

[41] Q. Jin, F. Ren, D. Dai, N. Sun, Y. Qian, P. Song, The causality between intestinal flora and allergic diseases: insights from a bi-directional two-sample Mendelian randomization analysis, Front. Immunol. 14 (2023) 1121273, https://doi.org/10.3389/fimmu.2023.1121273.

[42] L. Neshatian, The assessment and management of defecatory dysfunction: a critical appraisal, Curr. Opin. Gastroenterol. 34 (1) (2018) 31–37, https://doi.org/10.1097/MOG.0000000000000407.

[43] Z. Wu, S. Huang, T. Li, N. Li, D. Han, B. Zhang, Z.Z. Xu, S. Zhang, J. Pang, S. Wang, G. Zhang, J. Zhao, J. Wang, Gut microbiota from green tea polyphenol-dosed mice improves intestinal epithelial homeostasis and ameliorates experimental colitis, Microbiome 9 (1) (2021) 184, https://doi.org/10.1186/s40168-021-01115-9.

[44] J. Gao, K. Xu, H. Liu, G. Liu, M. Bai, C. Peng, T. Li, Y. Yin, Impact of the gut microbiota on intestinal immunity mediated by tryptophan metabolism, Front. Cell. Infect. Microbiol. 8 (2018) 13, https://doi.org/10.3389/fcimb.2018.00013.

[45] L. Cui, X. Guan, W. Ding, Y. Luo, W. Wang, W. Bu, J. Song, X. Tan, E. Sun, Q. Ning, G. Liu, X. Jia, L. Feng, Scutellaria baicalensis Georgi polysaccharide ameliorates DSS-induced ulcerative colitis by improving intestinal barrier function and modulating gut microbiota, Int. J. Biol. Macromol. 166 (2021) 1035–1045, https://doi.org/10.1016/j.ijbiomac.2020.10.259.

[46] Z. Wu, S. Huang, T. Li, N. Li, D. Han, B. Zhang, Z.Z. Xu, S. Zhang, J. Pang, S. Wang, G. Zhang, J. Zhao, J. Wang, Gut microbiota from green tea polyphenol-dosed mice improves intestinal epithelial homeostasis and ameliorates experimental colitis, Microbiome 9 (1) (2021) 184, https://doi.org/10.1186/s40168-021-01115-9.

[47] S. Fukuda, H. Toh, K. Hase, K. Oshima, Y. Nakanishi, K. Yoshimura, T. Tobe, J.M. Clarke, D.L. Topping, T. Suzuki, T.D. Taylor, K. Itoh, J. Kikuchi, H. Morita, M. Hattori, H. Ohno, Bifidobacteria can protect from enteropathogenic infection through production of acetate, Nature 469 (7331) (2011) 543–547, https://doi.org/10.1038/nature09646.

[48] A. Granito, P. Muratori, L. Muratori, Editorial: gut microbiota profile in patients with autoimmune hepatitis-a clue for adjunctive probiotic therapy? Aliment. Pharmacol. Ther. 52 (2) (2020) 392–394, https://doi.org/10.1111/apt.15795.